Carrington cycle 24: the solar chromospheric emission in a historical and stellar perspective

K.-P. Schröder,[1]⋆ M. Mittag,[2]⋆ J. H. M. M. Schmitt,[2]⋆ D. Jack,[1] A. Hempelmann[2] and J. N. González-Pérez[2]

[1]*Departamento Astronomia, Universidad de Guanajuato, A.P. 144, Guanajuato, GTO CP 36000, Mexico*
[2]*Hamburger Sternwarte, Universität Hamburg, Gojenbergsweg 112, D-21029 Hamburg, Germany*

ABSTRACT

We present the solar S-index record of cycle 24, obtained by the Telescopio Internacional de Guanajuato, Robotico Espectroscopico robotic telescope facility and its high-resolution spectrograph HEROS ($R \approx 20\,000$), which measures the solar chromospheric Ca II H&K line emission by using moonlight. Our calibration process uses the same set of standard stars as introduced by the Mount Wilson team, thus giving us a direct comparison with their huge body of observations taken between 1966 and 1992, as well as with other cool stars. Carrington cycle 24 activity started from the unusually deep and long minimum 2008/2009, with an S-index average of only 0.154, 0.015 deeper than the one of 1986 ($\langle S \rangle = 0.169$). In this respect, the chromospheric radiative losses differ remarkably from the variation of the coronal radio flux F10.7 cm and the sunspot numbers. In addition, the cycle 24 S-amplitude remained small, 0.022 (cycles 21 and 22 averaged: 0.024), and so resulted in a very low 2014 maximum of $\langle S \rangle = 0.176$ (cycles 21 and 22 averaged: 0.193). We argue that this find is significant, since the Ca II H&K line emission is a good proxy for the solar far-ultraviolet (far-UV) flux, which plays an important role in the heating of the Earth's stratosphere, and we further argue that the solar far-UV flux changes with solar activity much more strongly than the total solar output.

Key words: Sun: activity – Sun: chromosphere – stars: activity – stars: chromospheres – stars: solar-type.

1 INTRODUCTION

The period between approximately 1650 and 1715 has long been known for its paucity and/or absence of sunspots, first described by Spoerer (1890) and Maunder (1894). For a long time, it had been thought that this apparent absence of sunspots was due to a lack of suitable observations, until Eddy (1976) convincingly demonstrated that this apparent absence of sunspots was really an actual absence of sunspots and not merely an absence of observations; Eddy (1976) also introduced the name 'Maunder Minimum' for this period of time. Ever since, the question has centred around what made the Sun enter and eventually leave this 'Maunder Minimum' phase and what the properties of the Sun were at that time; unfortunately, except for sunspot numbers, no physical information is available from that period.

The current Carrington cycle 24 of the Sun follows the extraordinarily long and deep minimum of 2008/2009. Schröder et al. (2012) showed that there were 'zero-active' minimum days, when the chromospheric emission was at its entirely inactive, basal flux level. The Sun was entirely void of activity regions, not even showing plages or faculae, which are a common sight on a 'normal minimum', i.e. 'zero-sunspot' day, yet the random magnetic fine structure (unrelated to any magnetic activity region) is still present in those same days of zero activity and not reduced at all, as seen in the respective SOlar and Heliospheric Observatory (SOHO) images; as shown by Vögler & Schüssler (2007), it is a simple by-product of convection (dubbed 'local dynamo').

Various solar activity data suggest that the maximum of Carrington cycle 24 occurred in the second half of 2014. The cycle was remarkably weak and even in the maximum year, one day was recorded without any sunspots present on the solar surface (i.e. 2014 July 17). By now, the Sun has already gone well beyond its peak activity in the current cycle and is approaching a new minimum. It is therefore appropriate to put the current solar cycle in its proper historical and stellar perspective.

2 TIGRE-OBSERVATIONS OF SOLAR CHROMOSPHERIC ACTIVITY

2.1 Overview and context

We use our Telescopio Internacional de Guanajuato, Robotico Espectroscopico (TIGRE) 1.2-m robotic telescope located in

⋆ E-mail: kps@astro.ugto.mx (K-PS); mmittag@hs.uni-hamburg.de (MM); jschmitt@hs.uni-hamburg.de (JHMMS)

Guanajuato, central Mexico, and its HEROS spectrograph (spectral resolution ≈20 000, with a spectral coverage of ≈3800–8800 Å); this facility is described in detail by Schmitt et al. (2014).

For a consistent treatment of the echelle order sampling, assessment of their sensitivity functions, wavelength calibration and stray light removal, a data-reduction pipeline is used. The echelle order sampling parameters are recalibrated each time the spectrograph passes maintenance (typically once a year), while flat-fields, white-light and ThAr lamp emission line spectra are taken each night at least twice, before and after the observations. In addition, a spectrum of Vega or other suitable standard star is taken to get a reliable, yet only relative flux-calibration.

Lunar light is used to obtain full-disc solar (i.e. Sun as a star) spectra typically twice a week whenever possible. In this way, we study the Sun with the same equipment as used for a set of standard stars (and program stars of our stellar chromospheric activity survey), originally defined by O. C. Wilson (see Duncan et al. 1991; Baliunas et al. 1995, and references therein). Specifically, the surface area of the Moon sampled by the fibre of the adapter unit channelling the light in the TIGRE spectrograph has a size of 3 arcsec in diameter, and is thus only slightly larger than the average seeing disc of a star.

Consequently, we can directly compare the integrated solar emission to a huge body of stellar activity data gathered during the last five decades.

2.2 Definition of the S-index

The original Mount Wilson index is defined through the expression (Vaughan, Preston & Wilson 1978)

$$S_{\mathrm{MWO}} = \alpha \left(\frac{N_{\mathrm{H}} + N_{\mathrm{K}}}{N_{\mathrm{R}} + N_{\mathrm{V}}} \right), \tag{1}$$

where α is an instrument-dependent calibration factor, used to put data taken with different equipment on the same scale, N_{H} and N_{K} are the counts measured in a 1-Å-wide window, each centred on the Ca II H&K line cores, and N_{R} and N_{V} are the counts in two 20-Å-wide, 'quasi-continuum' reference bands centred on 3901 and 4001 Å, conveniently encompassing the two Ca II lines in between. In this way, any variable atmospheric opacity and its possibly variable slope in the near-ultraviolet (near-UV) automatically cancel out. In the original four-photomultiplier set-up used at Mount Wilson, the line-centred channels had an approximately triangular transmission profile, while we nowadays obtain digital records of spectra and use a rectangular profile; the small differences between the two are taken care of in the calibration process.

2.3 Calibration of the TIGRE S-index

For each instrumental set-up, including our TIGRE facility, the calibration process has to be carried out continuously and must be monitored carefully. For this purpose, TIGRE regularly observes a set of stars, listed in Baliunas et al. (1995) and Hall, Henry & Lockwood (2007) as a reference to all occurring levels of activity, and selected for their relative low degree of variation.

Here, we show results from two different observation campaigns and set-ups. The first campaign was undertaken in the 2008/2009 season with TIGRE still located at the Hamburg Observatory, then called Hamburg Robotic Telescope (HRT). The second campaign refers to the observations carried out at the La Luz Observatory since 2013. Therefore, we use two separate S-index calibrations to handle possible long-term instrumental drifts, such as residual
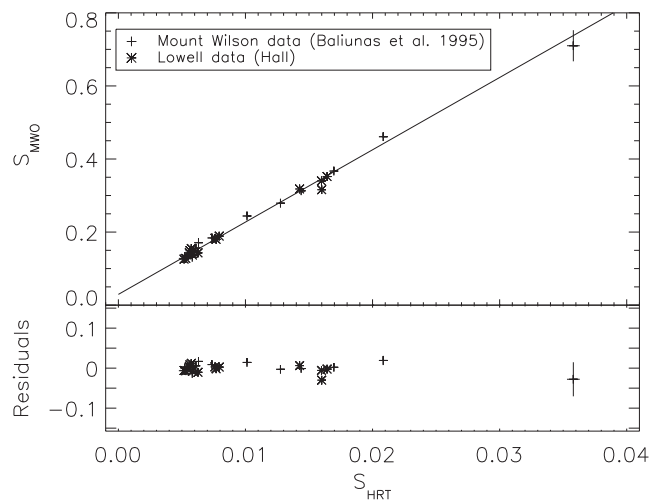

Figure 1. TIGRE S-index calibration for the observations taken in Hamburg in 2008/2009 (Mittag et al. 2011).
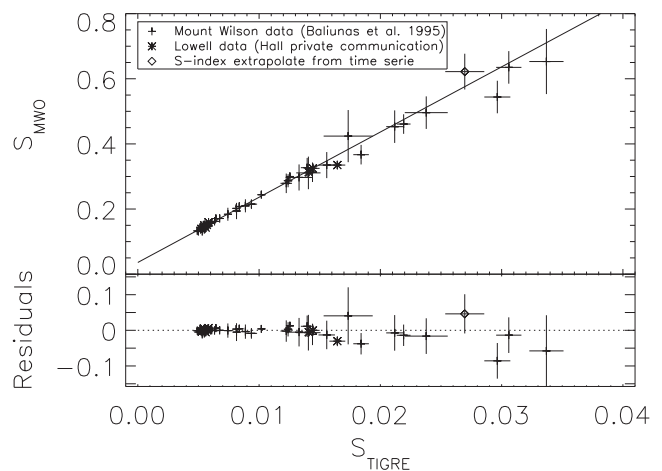

Figure 2. TIGRE S-index calibration for the La Luz data taken since 2013 (Mittag, Schmitt & Schröder 2016).

undercorrection or overcorrection for the echelle stray light in the line cores, which is accounted for with a zero-point small offset in the linear regression of TIGRE's raw S-values over the respective original Mount Wilson S-indices for our set of calibration stars. The calibration data for the period 2008/2009 are shown in Figs 1 and 2 for the data taken from La Luz data since 2013. It is obvious from both figures that a linear relation describes the transformation into the Mount Wilson scale very well; specifically, the calibration relation for 2008/2009 data is given by (cf. Mittag et al. 2011)

$$S_{\mathrm{MWO}} = (0.029 \pm 0.004) + (19.8 \pm 0.6)S_{\mathrm{HRT}} \tag{2}$$

and for the data taken since 2013 (cf. Mittag et al. 2016),

$$S_{\mathrm{MWO}} = (0.036 \pm 0.003) + (20.0 \pm 0.4)S_{\mathrm{TIGRE}}. \tag{3}$$

These relations are represented by a solid line in Figs 1 and 2 together with the fitted residuals. We note that especially at low activity levels (critical for the Sun in low activity states), the residuals are very small indeed because here the calibration stars show nearly no long-term variability. Furthermore, the slope of the regression is the same in both periods to within the errors, which demonstrates that the sample of calibration stars as a whole does not significantly vary over longer time-scales.
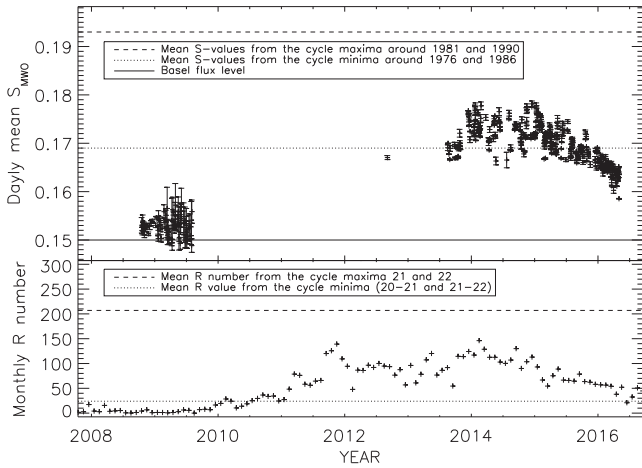
Figure 3. TIGRE's Mount Wilson-calibrated S-index values of the 2008/2009 (last activity minimum) and 2013–2016 period (error bars refer to measurement uncertainties only; calibration errors may reach 0.004), in perspective with previous average minimum and maximum activity (lines; see Section 4.1) and SIDC monthly sunspot numbers (below). The chromospheric emission of cycle 24 is much lower than in previous cycles.

2.4 TIGRE S-index of the Sun

In Fig. 3, we show the solar S-index measurements so far obtained with TIGRE. While our TIGRE observations of the past solar minimum in 2008/2009 were obtained from the preliminary telescope set-up at the Hamburg Observatory and published by Mittag et al. (2011) and Schröder et al. (2012), the maximum of Carrington cycle 24 was covered from 2013 August onwards, after the installation of TIGRE at the La Luz Observatory near Guanajuato. The best and simplest way to obtain the S-index of the Sun are observations of lunar light, where the Moon is used as a 'mirror' for the incident solar radiation. Such observations provide an unbiased measure of the light of the integral solar disc and therefore such spectra record 'the Sun as a star' with the disc-integration coming for free.

To test Olin Wilson's idea that the sunlight reflected by the Moon is a very good proxy for direct sunlight and to check how well our reduction pipeline deals with the echelle blaze functions, we compare the respective near-UV spectral range with the flux-calibrated, high-resolution KPNO FTS Solar Flux Atlas (see http://kurucz.harvard.edu/sun/fluxatlas/fluxatlastext.tab). This atlas provides a very high signal-to-noise ratio spectrum of integrated sunlight with a spectral resolution of several hundred thousand. Furthermore, the FTS stray light and resulting solar spectrum dynamics are very well calibrated, and in the near-UV, the residual uncertainty is believed to be 0.2 per cent.

In Fig. 4, we compare the TIGRE lunar spectra (black histograms) with the corresponding FTS spectra (red histograms) for the four spectral ranges (V, K, H, R) relevant for the S-index determination; note that the much higher spectral resolution FTS data were 'blurred' to the TIGRE resolution of ∼20 000. Fig. 4 shows that the spectra agree very well, and outside the cores of the Ca II lines, we find variations between our moonlight spectra and the FTS direct sunlight spectrum of under 1–2 per cent, which appear on short scales and which we attribute to our broadening procedure. In the cores of the Ca II H&K lines, the FTS spectra are at a much higher level, which is not surprising given that they were taken at the time of solar maximum.

We therefore conclude that our TIGRE Moon spectra represent a very good approximation to the 'true' solar spectrum in the Ca II
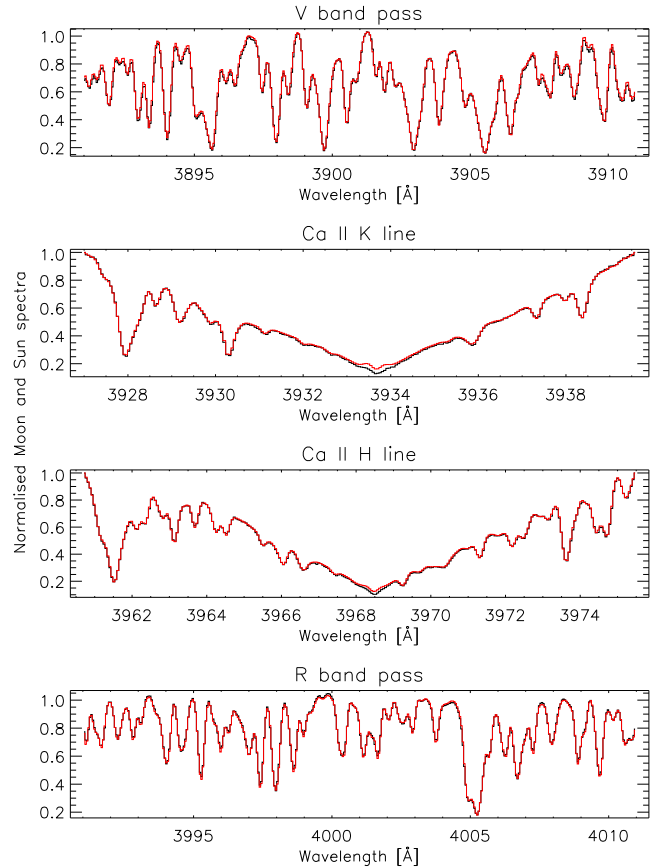

Figure 4. Comparison of a solar KPNO FTS spectrum (red; reduced to a spectral resolution of 20 000 for better comparability) and a TIGRE moon-light spectrum (black) in the spectral range relevant for the S-index measurements; see the text for details.

region, and consequently, our determinations of the solar S-index should have a very small systematic error at worst. Since – a benefit of our approach – we use the same equipment and calibration for the Sun and for the stars, there is no instrumental or methodological bias at all and consequently, the solar chromospheric activity recorded by means of the Mount Wilson S-index is *directly* comparable with the S-index records of stars.

The method described above has been used for the data taken since 2013 at the La Luz site. However, in the observations taken in 2008/2009 at Hamburg, only two direct Moon spectra could be obtained. The majority of the Hamburg observations uses sky-scattered sunlight. The physical processes involved in sunlight scattering include Rayleigh scattering, Mie scattering, as well as rotational Raman scattering off the N_2 and O_2 molecules in the Earth's atmosphere. The latter process is particularly relevant for our Ca II H&K data, since it leads to the so-called 'Ring effect', first described by Grainger & Ring (1962). Rotational Raman scattering is inelastic, leading to a frequency redistribution of the scattered light, which leads to a fill-in of the stronger solar lines from the adjacent continuum. Specifically, for the Ca II H&K lines, the Ring effect reaches well over 1 per cent of the solar continuum intensity and will therefore strongly affect the measurement of the S-index; for a more recent, quantitative study of the Ring effect, we refer to Sioris et al. (2002).

The Ring effect is naturally also present in the 2008/2009 TIGRE data. In Fig. 5, we compare a solar spectrum (of the core of the Ca II K line) taken from the Moon and from the day sky (left-hand panel)
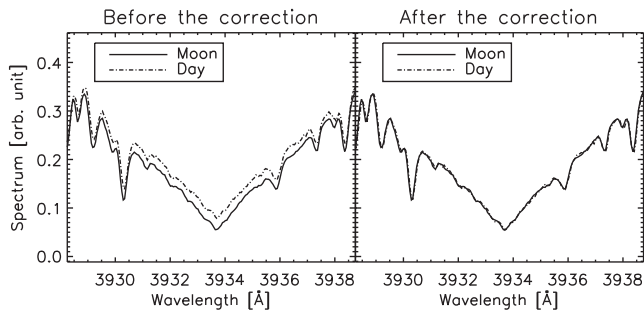
Figure 5. Moon and sky-scattered sunlight spectra before and after the scattering correction.

and demonstrate that our scattering corrections removes the Ring effect (right-hand panel). We normalize the sky-scattered sunlight Ca II K line profile by the deeper profile obtained from the direct sunlight obtained from the Moon spectra; our resultant correction of the sky-scattered sunlight spectra is of the same order as predicted by the modelling of Sioris et al. (2002).

2.5 Further S-data sets

The gap in time between the original Mount Wilson S-measurements and our TIGRE measurements has been filled by several initiatives, most notably from Lowell Observatory (J. Hall and colleagues) and the National Solar Observatory (NSO). However, the different calibration and instrumental issues still need a more detailed debate than the one we can give below.

Using the late Mount Wilson, NSO/Sacramento Peak, Lowell and Lick S-values, Egeland et al. (2016) find that cycle 23 was already quite weak, deriving maximum and minimum S-values of 0.178 and 0.163, respectively. Inspecting their full data set of S-index values, which is provided online and also covers cycle 24, we find good agreement with our S-index values for the time since 2013. However, for the past minimum, their S-index values are larger than ours, while their S-index values for the early 1990s (cycle 22) are systematically lower than the measurements presented by Baliunas et al. (1995), to which we calibrated our S-index values shown in Fig. 3.

Egeland et al. (2016) argue that our TIGRE measurements taken in 2008/2009 are affected by an incorrect correction for the Ring effect described above. However, first, we argue that our corrections are correct, and secondly, we point out the S-index values obtained from two direct moonlight spectra (without any Ring effect) in 2008 are also low. In addition, the S-index time series presented by Egeland et al. (2016) does not appear to reflect, what is shown by all other solar activity indicators (see Sections 2.6 and 3: SOLIS Ca II K 1-Å, radio flux, sunspot numbers), that the 2008/2009 minimum is lower than the minima in 1986 and 1997.

Further evidence is available from the fact that the Sun is the only star with a directly observable surface. Egeland et al. (2016) inspected SOHO MDI magnetograms on two specific dates (1997 January 28 and 2009 October 9), since for both days, they obtain relatively low S-index values of 0.1593 and 0.1596, respectively. The first value was measured with the original Mount Wilson HKP-2 instrument, while the second value was transformed from the NSO/Sacramento Peak Ca II K 1-Å emission index. While Egeland et al. (2016) state that they find a low activity on either day, a closer inspection of the MDI magnetogram from 1997 January 28 (see Fig. 6) reveals the presence of a small region of chromospheric activity, while, in contrast, on 2009 October 9, the Sun was entirely
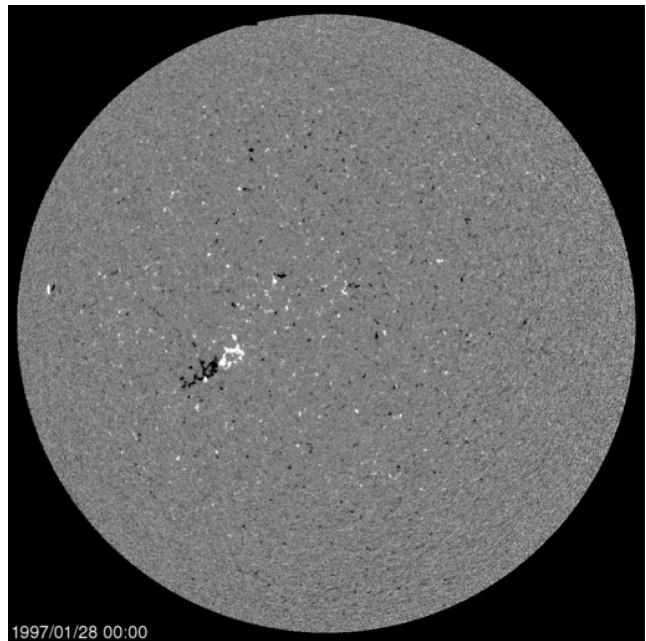

Figure 6. SOHO MDI magnetogram from 1997 January 28 (https://sohodata.nascom.nasa.gov/cgi-bin/data_query).

Figure 7. SOHO MDI magnetogram from 2009 March 8 (https://sohodata.nascom.nasa.gov/cgi-bin/data_query).

void of any activity. Yet, the S-index quoted by Egeland et al. (2016) for that day is not any lower than the one measured by Mount Wilson for the slightly active day, 1997 January 28.

We carried out the same exercise for 2009 March 8, since on this day, we obtained one of the two moonlight spectra from Hamburg with a very low S-index of 0.152 ± 0.006. In Fig. 7, we show the respective SOHO MDI magnetogram taken on that day, and just as is the case for 2009 October 9, there is absolutely no activity region visible on the surface. By this admittedly limited but yet very representative probe, our S-index values appear to be consistent with the Mount Wilson measurements during the past minimum period.
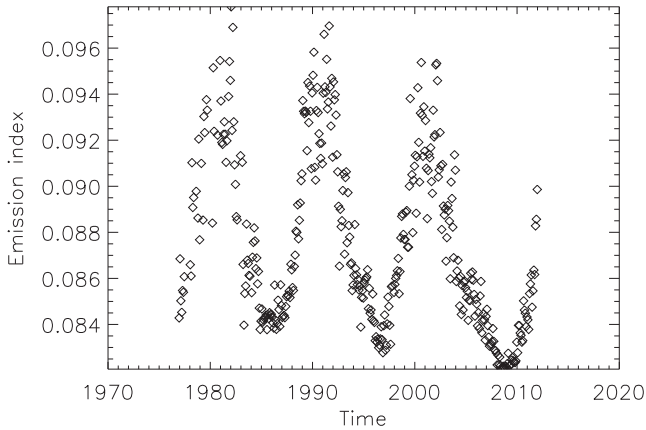
Figure 8. Monthly medians of the SOLIS-calibrated Ca II K 1-Å index time series of the NSO (source: data made available by Bertello et al. 2017).

2.6 Other solar data sets

In the mid-1970s, the NSO began taking regular observations of the disc-integrated solar Ca II K line at Sacramento Peak, measuring, in particular, the so-called 1-Å Ca II K emission index, defined as the equivalent width of a band with a width of 1 Å centred on the K-line core. After 2015 October 1, the measurements were continued using the Integrated Sunlight Spectrometer (ISS) on the Synoptic Optical Long-term Investigations of the Sun (SOLIS) facility. The ISS has actually been in operation since late 2006 at NSO/Kitt Peak, so that there is an overlap of about 8 yr between the two time series.

Interestingly, the two time series differ, and Bertello, Marble & Pevtsov (2017) provide a detailed discussion of these discrepancies and develop a procedure to unify the two time series. Specifically, Bertello et al. (2017) correct the NSO/Sacramento Peak measurements and empirically rescale them to the SOLIS data, which are not affected by sky-scattered light and the aforementioned Ring effect. In Fig. 8, we show the monthly medians of their re-calibrated data; obviously, the minimum in NSO 1-Å Ca II K emission index time series is clearly lower in 2008/2009 than in the minimum in 1997, consistent with the TIGRE S-index data. Unfortunately, SOLIS is not able to measure the S-index directly and cannot perform measurements of stars; therefore, the stellar dimension is missing from those measurements.

3 SOLAR ACTIVITY DURING CARRINGTON CYCLE 24

The last solar minimum and the ongoing Carrington cycle 24 are unusual not only with respect to the solar UV emission, but also in many respects, which we briefly demonstrate in this section.

3.1 Radio emission and sunspot number

To provide a wider context, we show in Fig. 9 the monthly averaged sunspot numbers (upper panel, taken from the Belgian SIDC website) for the Carrington cycles 20–24 and values of the F10.7-cm radio flux (medium panel, NR Canada website). One recognizes, first, the very close correlation between these so different activity indicators, and, secondly, that in the present cycle 24 maximum, both these indicators reached only half of their levels of the maxima of 1980 and 1991, or about their level of early 2003.
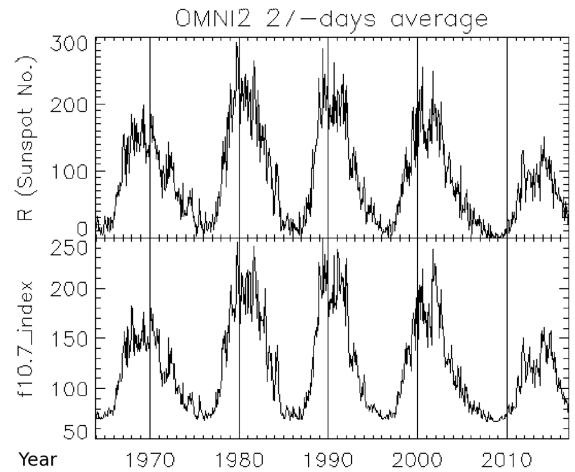

Figure 9. 27 day averages of: Upper panel: SIDC (new) sunspot number; lower panel: NRC F10.7-cm coronal radio flux (source: OMNI/NASA).

3.2 Total solar irradiance

The total solar irradiance (TSI) has been continuously monitored by various space-based instruments since 1978. Since the zero-points of the individual instruments do not fully agree, it is a non-trivial task to combine the results of different missions into a definitive record of the solar TSI. BenMoussa et al. (2013) and Fröhlich (2012) discuss the various problems in extensive detail and provide a summary of the TSI measurements during the last three cycles (i.e. Carrington cycles 21–23). As discussed by Fröhlich (2012), even the TSI may have dropped during the 2008/2009 minimum below the TSI values recorded during any of the previous minima, albeit only by a very small margin, probably smaller than ΔTSI/TSI $\approx (10^{-4})$, but long-term drifts and calibration differences between the different TSI missions prevent the derivation of more accurate numbers.

3.3 Far-UV emission

We next use the SOLSTICE data of the SORCE mission, provided by the Laboratory for Atmospheric and Space Physics (LASP) of the University of Colorado. These far-UV spectral irradiance measures are of special interest, because a 'haze' of metal lines (Anderson & Athay 1989) should reveal magnetic chromospheric heating by radiative losses, similar to the S-index, and like the latter, SOLSTICE data are star-calibrated, with the consequence that they do *not* suffer from calibration lamp and/or electronics degradation problems (see the discussion by Lockwood 2013, and references therein).

We integrate spectral irradiance over the wavelength range of 200–280 nm, which by wavelength and intensity is the relevant spectral window for stratospheric warming by photodissociation of molecules such as ozone and show (in Fig. 10) the averages obtained for periods of half a year, to minimize the impact of short-term fluctuations of the solar activity, covering the time-span of 2003 to 2016. Although this mission missed the maximum of cycle 23 by two years, it is evident from Fig. 10 that the maximal far-UV irradiation in cycle 24 is, like the S-index, again exceptionally low. With a total variation of only 1.4 per cent, the cycle 24 maximum level compares with the cycle 23 decline of late 2004. That is about 1 per cent lower than the far-UV irradiation of early 2003, with which time the cycle 24 maxima of F10.7 and sunspot numbers compare.
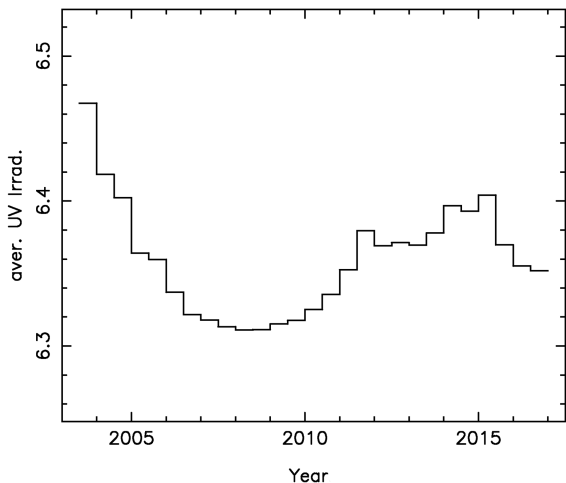
Figure 10. SOLSTICE/SORCE integrated spectral irradiance of the far-UV 200–280-nm window, relevant for stratospheric warming by photodissociation of molecules, averaged over periods of half a year between 2003 and 2016. The maximum of the present 24th cycle appears equally reduced as observed in TIGRE S-index time series calibrated to the Mount Wilson scale.
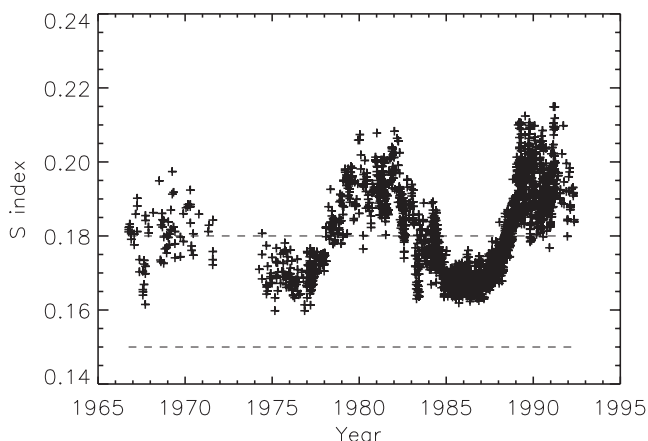

Figure 11. Historical solar Mount Wilson S-index values, covering the solar chromospheric activity from the 1960s to the 1990s, according to Baliunas et al. 1995. Horizontal lines mark extreme TIGRE S-index values of cycle 24.

4 THE HISTORICAL SOLAR AND STELLAR PERSPECTIVE

4.1 The solar perspective

The hitherto most complete description of the Mount Wilson H&K monitoring project was presented by Baliunas et al. (1995). Recently, these data have become publicly available, covering the period of 1966–1992 with rather unequal but sufficient sampling of the chromospheric activity maxima of 1980 and 1991 (S-index of 1-yr averages around maxima: 0.193, extreme: 0.215), as well as of the minimum in 1986 (between cycles 21 and 22, S-index 1-yr average: 0.169, extreme: 0.162). Superimposed in Fig. 11, we plot (with dashed lines) the extreme S-index values observed by TIGRE in 2008 and 2014, i.e. 0.150 and 0.180 (cf. Fig. 3).

We therefore conclude that the minimum in 2008 (average: 0.154) reached significantly below the minimum of 1986 (by 0.015 in 1-yr averages), and the cycle 24 maximum observed by TIGRE (S-index
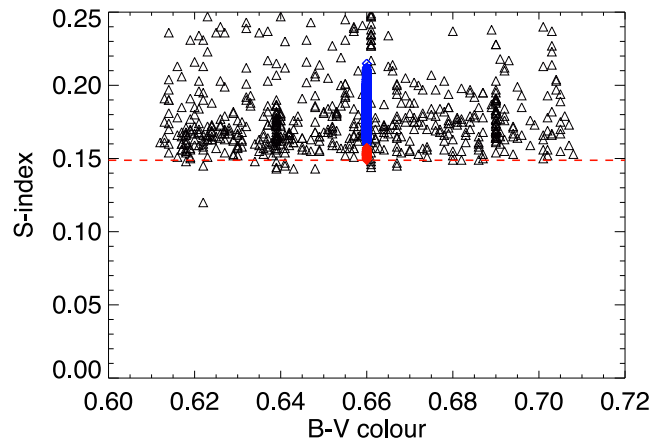

Figure 12. Stellar S-index values (triangles, taken from Mittag et al. 2013) in the colour range of 0.61–0.71, together with the solar S-index values shown in Fig. 11 (blue filled symbols over $B-V = 0.66$) and Fig. 3 (red symbols); the red dashed line marks the lowest TIGRE measured S-indices.

1-yr average of 0.176) is much lower (by 0.017) than the cycle 22 maximum; it is in fact closer to the minimum of 1986.

Hence, the change is not so much a smaller cycle 24 S-index amplitude between the 1-yr averages around maximum and minimum (0.022, as compared to 0.024 in cycles 21 and 22). Rather, chromospheric activity has now settled for a 0.015 deeper starting level. This is what makes the S-index underscore, on a relative scale, what the already low cycle 24 records of sunspot numbers and F10.7-cm flux let expect.

4.2 The stellar perspective

We next move on to the stars and compare – in Fig. 12 – the solar S-index values reported by Baliunas et al. (1995; blue data points) and our TIGRE S-indices (cf. Fig. 3, red data points) with a larger number of S-index measurements of solar-like stars (taken from Mittag et al. 2013, triangular data points). Clearly, the TIGRE values reproduce very well the lower cut-off (at around 0.15), already observed for solar-like stars by Duncan et al. (1991). We are therefore confident that our TIGRE calibration is accurate, especially for stars of relatively low activity, and argue that during the extended solar minimum in 2008/2009 the Sun was actually close to the minimal S-index values observed for solar-like stars and hence very close to the state it had during the 'Maunder Minimum' period.

5 DISCUSSION AND CONCLUSIONS

The now outgoing Carrington cycle 24 is not only much weaker than its three predecessors in terms of sunspot numbers and F10.7-cm coronal radio flux (see Fig. 9), the average S-index of chromospheric emission was even more reduced. According to our TIGRE observations presented here, its amplitude between 1-yr averages of the S-index measurements was only 0.022 (rather than 0.024, which was typical of cycles 21 and 22). Most remarkably, however, the activity cycle started from a minimum deeper by 0.015 (see Fig. 11), meaning that the extraordinary decrease of the S-index has a time-scale longer than a single cycle.

The same behaviour is seen in the averaged, integrated spectral far-UV flux in the wavelength range 200–280 nm (cf. Fig. 10), according to the star-calibrated SOLSTICE/SORCE data available for the time-span of 2003 to 2016. Importantly, in both, the cycle 24 minimum (cf. Lockwood 2013) and maximum (compare Fig. 3 with Fig. 2) far-UV irradiation is lower by about 1 per cent against

the projected cycle variation of the F10.7 cm and sunspot number records. The cycle 24 amplitude of the far-UV averaged irradiation is 1.4 per cent.

By simple comparison, we find that S-index and far-UV irradiation cycle variations scale approximately to 0.016 in S-index being equivalent to 1 per cent in far-UV irradiation, making the former index a very good proxy for the latter – not requiring space-based instrumentation and having a longer track record. We extrapolate, that in cycles 21 and 22 maxima, the average far-UV irradiation must have been almost 3 per cent larger than in 2008, while in the respective minima it was still 1 per cent larger.

Such a lasting deficiency of the solar UV irradiance implies a decline of the magnetic chromospheric heating that lasts beyond the present cycle, thus providing further evidence that the Sun is entering again into a grand minimum phase. In fact, such low activity could even been seen as the return to a long-term normal, since the two closest solar twins compare better, by their S-index values, with the low cycle 24 solar chromospheric activity (see Mittag et al. 2016).

In the context of possible TSI changes, we also analysed how much variance of the latter would be needed to produce a 1 per cent drop of the far-UV flux of the Sun, using PHOENIX model atmospheres (Hauschildt, Allard & Baron 1999) with a very small difference in effective temperature. We find that, driven by the large UV opacities, a hypothetical decrease of the solar T_{eff} of as little as 1.5 K over the decade or so in question would already account for such an additional 1 per cent decrease of the far-UV irradiation. However, this would also imply a drop in TSI by about 0.1 per cent, probably more than observational evidence seems to suggest. Hence, we consider it more plausible that the decrease of the far-UV irradiation and Ca II line emission is entirely due to a long-term reduced magnetic heating, which is consistent with only a small extra decrease in the TSI during the past minimum.

The evidence presented here suggests that a phase of reduced solar activity (or grand minimum) has an effect mainly on the solar far-UV emission, but much less so on the TSI. That would explain (see also the discussion by Ermolli et al. 2013), why on the one hand there is only inconclusive evidence for a global cooling during the Maunder and Dalton minima but, on the other hand, there was a clear rise in the frequency of cold northern winters (as shown by Ineson et al. 2011), which point to a then weaker jetstream and winter blocking situations.

The hypothesis, albeit not yet reproduceable in global climate models, is that the above far-UV spectral range ($\approx$200–280 nm) is responsible for the photodissociation of molecules in the Earth's stratosphere and constitutes its main radiative heating. Temperatures there are related to the strength and behaviour of the jetstream (by climate sciences referred to as NAO, North Atlantic Oscillation). Consequently, low solar activity and lower stratospheric temperatures seem to, statistically, favour a weaker jetstream with wider oscillations (see Ineson et al. 2011, and references therein), subtly allowing for more pronounced blocking situations in the Northern hemisphere. A rise of colder-than-average winters during times of low solar activity is simply caused by the formation of more large, persistent bubbles of arctic air – without much affecting average world temperatures.

In this context, we need consistent chromospheric emission records over long periods, in order to test refined climate models and to obtain a clearer correlation with climate records. Since direct, well-calibrated observations of the far-UV flux only exist for about two decades at best, the longer time-span available

with the solar Mount Wilson-calibrated S-index records provide an important advantage. O. C. Wilson's star-calibrated method makes present and future records directly comparable with those obtained over half a century ago, and with TIGRE we will continue the spectroscopic monitoring of solar and stellar chromospheric activity.

REFERENCES

Anderson L. S., Athay R. G., 1989, ApJ, 346, 1010
Baliunas S. L. et al., 1995, ApJ, 438, 269
BenMoussa A. et al., 2013, SoPh, 286, 289
Bertello L., Marble A. R., Pevtsov A. A., 2017, preprint (arXiv:1702.00838)
Duncan D. K. et al., 1991, ApJS, 76, 383
Eddy J. A., 1976, Science, 192, 1189
Egeland R., Soon W., Baliunas S., Hall J. C., Pevtsov A. A., Bertello L., 2016, AJ, 835, 25
Ermolli I. et al., 2013, Atmos. Chem. Phys., 13, 3945
Fröhlich C., 2012, Surv. Geophys., 33, 453
Grainger J. R., Ring J., 1962, Nature, 193, 762
Hall J. C., Henry G. W., Lockwood G. W., 2007, AJ, 133, 2206
Hauschildt P. H., Allard F., Baron E., 1999, ApJ, 512, 377
Ineson S. et al., 2011, Nat. Geosci. Lett., NGEO1282
Lockwood M., 2013, J. Geophys. Res., 116, D16103
Maunder E. W., 1894, PASP, 6, 125
Mittag M., Hempelmann A., González-Pérez J. N., Schmitt J. H. M. M., Hall J. C., 2011, ASPC, 448, 1187
Mittag M., Schmitt J. H. M. M., Schröder K.-P., 2013, A&A, 549, A117
Mittag M., Schröder K.-P., Hempelmann A., González-Pérez J. N., Schmitt J. H. M. M., 2016, A&A, 591, A89
Schmitt J. H. M. M. et al., 2014, Astron. Nachr., 335, 787
Schröder K.-P., Mittag M., Pérez Martínez M. I., Cuntz M., Schmitt J. H. M. M., 2012, A&A, 540, A130
Sioris C. E., Evans W. F. J., Gattinger R. L., McDade I. C., Degenstein D. A., Llewellyn E. J., 2002, Can. J. Phys., 80, 483
Spoerer F. W. G., 1890, Astron. Nachr., 124, 107
Vaughan A. H., Preston G. W., Wilson O. C., 1978, PASP, 90, 267
Vögler A., Schüssler M., 2007, A&A, 465, L43

This paper has been typeset from a TEX/LATEX file prepared by the author.